RAD Conference Proceedings, vol. 9, pp. 7-12, 2025
ISSN 2466-4626 (online) | DOI: 10.21175/RadProc.2025.02
www.rad-proceedings.org

NON-LINEAR VISCOELASTIC BEAMS WITH TWO-DIMENSIONAL MATERIAL INHOMOGENEITY: A LONGITUDINAL FRACTURE ANALYSIS

Victor Rizov*

University of Architecture, Civil Engineering and Geodesy, Sofia, Bulgaria

Abstract. *This paper is focussed on analysis of longitudinal fracture in non-linear viscoelastic beam structures with two-directional continuous material inhomogeneity (the material properties change continuously in both width and thickness directions). The viscoelastic model that is used for treating the mechanical behaviour of the beam represents a combination of four linear and two non-linear springs and dashpots. The model is under strains which change with time. The material properties involved in the constitutive law are distributed continuously in the cross-section. The strain energy release rate (SERR) is derived. For this purpose, the curvatures are determined by using the equilibrium equations. The method of the J-integral confirms the correctness of the SERR solution.*

Keywords: *Non-linearity, Viscoelastic behavior, Longitudinal Crack, Two-dimensional Inhomogeneity*

1. Introduction

The structural design has to assure that the engineering structures are capable of performing their intended functions. At the same time, the designed structures have to be economical. These contradictory goals put high requirements towards the engineering materials used. One of the advanced and efficient types of materials is the continuously inhomogeneous engineering materials. The properties of continuously inhomogeneous materials change smoothly in a structural member. The functionally graded materials are modern continuously inhomogeneous materials which have been widely in recent decades [1] - [3]. Graded distribution of material properties of functionally graded materials is formed by changing smoothly the composition of constituent materials in one or more directions in solid [4] – [6]. The concept of functionally graded materials is used for design of structural members with superior properties. Therefore, the functionally graded materials continue to replace the conventional homogeneous materials in some important structures in various engineering applications [7] – [9]. Various methods including a p-version finite element method are used to analyze inhomogeneous materials and structures [10], [11].

One of the challenging problems in the fracture behavior of continuously inhomogeneous (functionally graded) materials is the high probability of appearance of longitudinal cracks since these materials can be built-up layer by layer [12] – [14]. It is obvious that longitudinal cracks may affect the structural integrity and even may cause a structural failure.

An important factor with significant effect on fracture in continuously inhomogeneous materials is the viscoelastic behavior [15] – [17].

A crack problem in a functionally graded material of viscoelastic behavior is studied in [15]. The materil is with general material properties. To analyze the crack, the material is modeled by using a multi-layered model assuming that the variation of properties in each layer may be presented by exponential functions. Influence of various parameters on the fracture is studied.

Fracture in a double cantilever beam exhibiting viscoelastic behavior is thoroughly studied in [16]. The beam is under a pure moment applied in the end section. The two arms of the longitudinal crack have the same thickness. Effects of viscoelastic deformation on fracture are discussed.

Multiple fracture behavior of a functionally graded strip with viscoelastic properties is analyzed in [17]. The influence of such factors as crack length, distance between cracks, viscoelastic behavior and loading conditions on fracture is investigated.

The goal of this paper is to analyze longitudinal fracture in a non-linear viscoelastic beam structure that exhibits two-directional material inhomogeneity (the material properties change continuously along the width and thickness of the structure). The beam is under strains which change smoothly with time. The circumstance that factors such as two-dimensional inhomogeneity, non-linear viscoelastic behavior, and time dependence of strains imposed on the beam are considered jointly constitutes the novelty of this paper. The importance of the examined problem lies in the fact that in recent years there has been an increased interest in materials with two-directional inhomogenity [10]. This creates a need to conduct studies on the longitudinal failure of these materials in order to ensure the safe functioning of structures. In this paper, the SERR is derived by using a non-linear viscoelastic model for describing the mechanical behavior of the beam. The J-integral is applied for

* E-mail of the corresponding author: v_rizov_fhe@uacg.bg

check-up. The effect of various parameters on the SERR is assessed.

2. Model formulation

The non-linear viscoelastic mechanical model in Fig. 1 has four linear components (two springs with modules of elasticity, E_1 and E_2, and two dashpots with coefficients of viscosity, η_1 and η_2) and two non-linear components (a spring with modulus of elasticity, E_3, and a dashpot with coefficient of viscosity, η_3). The model is under strain, ε, that changes with time, t, according to the following law:

$$\varepsilon = v_{\varepsilon} t^2 , \tag{1}$$

where v_{ε} is a parameter that controls the change. It should be noted that models presenting various combinations of springs and dashpots are widely used when dealing (on theoretical level) with viscoelastic behavior.

The modulus of elasticity of the non-linear spring and the coefficient of viscosity of the non-linear dashpot change with strain according to the following dependences:

$$E_3 = E_0 - \beta\varepsilon , \tag{2}$$

$$\eta_3 = \eta_0 - \delta\varepsilon , \tag{3}$$

where parameters, β and δ, control the change. The physical motivation for adopting strain-dependent elastic modulus and viscosity coefficient in the form presented in Eqs. (2) and (3) lies in the fact that the elastic modulus and viscosity coefficient decrease with increasing strain due to material nonlinearity.

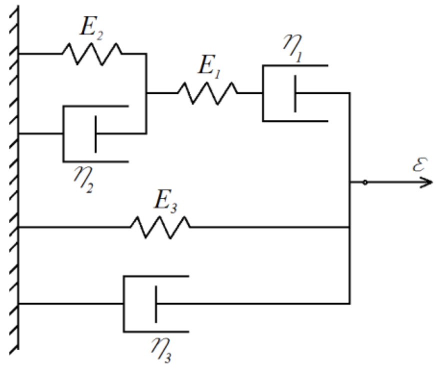

Figure 1. Non-linear viscoelastic mechanical model

In order to derive the stress-strain-time relationship of the model in Fig. 1, first, the mechanical response of the linear components is analyzed. For this purpose, the following dependences are written (Fig. 1):

$$\varepsilon_{E_1} + \varepsilon_{\eta_1} + \varepsilon_{E_2} = \varepsilon , \tag{4}$$

$$\varepsilon_{\eta_2} = \varepsilon_{E_2} , \tag{5}$$

$$\sigma_{E_1} = \sigma_{\eta_1} , \tag{6}$$

$$\sigma_{E_2} + \sigma_{\eta_2} = \sigma_{\eta_1} , \tag{7}$$

$$\sigma_{E_1} = \varepsilon_{E_1} E_1 , \tag{8}$$

$$\sigma_{E_2} = \varepsilon_{E_2} E_2 , \tag{9}$$

$$\sigma_{\eta_1} = \dot{\varepsilon}_{\eta_1} \eta_1 , \tag{10}$$

$$\sigma_{\eta_2} = \dot{\varepsilon}_{\eta_2} \eta_2 , \tag{11}$$

where ε_{E_1}, ε_{E_2}, ε_{η_1} and ε_{η_2} are the strains in the linear springs with modules of elasticity, E_1 and E_2, and in the linear dashpots with coefficients of viscosity, η_1 and η_2, respectively. The corresponding stresses are denoted by σ_{E_1}, σ_{E_2}, σ_{η_1} and σ_{η_2}, respectively. It should be mentioned that $\dot{\varepsilon}_{\eta_1}$ and $\dot{\varepsilon}_{\eta_2}$ are the time derivatives of the strains. By combining of (1), (4) – (11) and after some mathematical transformations, one obtains

$$\ddot{\varepsilon}_{E_2} + \theta_1 \dot{\varepsilon}_{E_2} + \theta_2 \varepsilon_{E_2} = \theta_3 t , \tag{12}$$

where

$$\theta_1 = \frac{E_2}{\eta_2} + \frac{E_1}{\eta_1} + \frac{E_1}{\eta_2} , \tag{13}$$

$$\theta_2 = \frac{E_1 E_2}{\eta_1 \eta_2} , \tag{14}$$

$$\theta_3 = \frac{2 v_{\varepsilon} E_1}{\eta_2} . \tag{15}$$

Equation (12) is solved as

$$\varepsilon_{E_2}(t) = \frac{B_{\phi}\rho_2 - A_{\phi}}{\rho_1 - \rho_2} e^{\rho_1 t} + \\ + \frac{A_{\phi} - B_{\phi}\rho_1}{\rho_1 - \rho_2} e^{\rho_2 t} + A_{\phi} t + B_{\phi} , \tag{16}$$

where

$$A_{\phi} = \frac{\theta_3}{\theta_2} , \tag{17}$$

$$B_{\phi} = -\frac{\theta_1 \theta_3}{\theta_2^2} , \tag{18}$$

$$\rho_1 = -0.5\theta_1 + \rho_3 , \tag{19}$$

$$\rho_2 = -0.5\theta_1 - \rho_3 , \tag{20}$$

$$\rho_3 = 0.5\left(\theta_1^2 - 4\theta_2\right)^{0.5} . \tag{21}$$

The conditions for expressing the first two coefficients in the exact form that appears in Eq.(16) are that at $t = 0$ the strain, ε_{E_2}, and its first derivative are zero.

The stress, $\sigma(t)$, in the model in Fig. 1 is determined as

$$\sigma(t)=\sigma_{E_2}(t)+\sigma_{\eta_2}(t)+\sigma_{\eta_3}(t)+\sigma_{E_3}(t), \quad (22)$$

where the stresses in the non-linear spring and dashpot, $\sigma_{E_3}(t)$ and $\sigma_{\eta_3}(t)$, are found as

$$\sigma_{E_3}(t)=E_3\varepsilon, \quad (23)$$

$$\sigma_{\eta_3}(t)=\eta_3\dot{\varepsilon}. \quad (24)$$

Here, E_3 and η_3 are determined by (2) and (3), respectively.

By using of (9), (11), (16), (22), (23) and (24), one derives

$$\sigma(t)=\varepsilon E_2\frac{B_1\rho_2-A_1}{\rho_1-\rho_2}e^{\rho_1 t}+ +\varepsilon E_2\frac{A_1-B_1\rho_1}{\rho_1-\rho_2}e^{\rho_2 t}+\varepsilon E_2 A_1 t+\varepsilon E_2 B_1+ +\varepsilon\eta_2\frac{(B_1\rho_2-A_1)\rho_1}{\rho_1-\rho_2}e^{\rho_1 t}+ +\varepsilon\eta_2\frac{(A_1-B_1\rho_1)\rho_2}{\rho_1-\rho_2}e^{\rho_2 t}+\varepsilon\eta_2 A_1+ +(E_0-\beta\varepsilon)\varepsilon+\frac{2}{t}(\eta_0-\delta\varepsilon)\varepsilon, \quad (25)$$

where

$$A_1=\frac{2E_1}{\eta_2\theta_2 t^2}, \quad (26)$$

$$B_1=-\frac{2E_1\theta_1}{\eta_2\theta_2^2 t^2}. \quad (27)$$

The constitutive law (25) of the model in Fig. 1 represents a non-linear dependency between stress, strain and time. This dependency is applied for modeling the mechanical behavior of the non-linear viscoelastic cantilever beam configuration (Fig. 2). b, h and l are the width, thickness and length of the beam, respectively. There is a longitudinal crack of length, a, in the beam. The widths of the crack arms are b_1 and b_2. The crack arm *1* is subjected to tension in its free end so as the axial displacement, u, changes with time according to the following law:

$$u=v_g t^2, \quad (28)$$

where v_g is a parameter that controls the change. Crack arm *2* is not loaded.

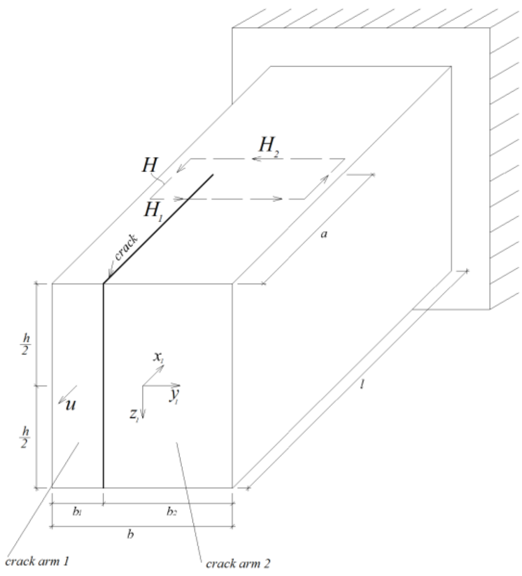

Figure 2. Non-linear viscoelastic beam with a longitudinal crack

The beam (Fig. 2) exhibits two-directional continuous material inhomogeneity in its cross-section, i.e. the material properties are continuous functions of both y_1 and z_1 coordinates. The change of modules of elasticity and the coefficients of viscosities is

$$E_1=E_{gl1}e^{\mu_1\left(\frac{\frac{h}{2}+z_1}{h}+\frac{\frac{b}{2}+y_1}{b}\right)}, \quad (29)$$

$$E_2=E_{gl2}e^{\mu_2\left(\frac{\frac{h}{2}+z_1}{h}+\frac{\frac{b}{2}+y_1}{b}\right)}, \quad (30)$$

$$\eta_1=\eta_{gl1}e^{\mu_3\left(\frac{\frac{h}{2}+z_1}{h}+\frac{\frac{b}{2}+y_1}{b}\right)}, \quad (31)$$

$$\eta_2=\eta_{gl2}e^{\mu_4\left(\frac{\frac{h}{2}+z_1}{h}+\frac{\frac{b}{2}+y_1}{b}\right)}, \quad (32)$$

$$E_0=E_{glo}e^{\mu_5\left(\frac{\frac{h}{2}+z_1}{h}+\frac{\frac{b}{2}+y_1}{b}\right)}, \quad (33)$$

$$\eta_0=\eta_{glo}e^{\mu_6\left(\frac{\frac{h}{2}+z_1}{h}+\frac{\frac{b}{2}+y_1}{b}\right)}. \quad (34)$$

In formulae (29) – (34), E_{gl1}, E_{gl2}, η_{gl1}, η_{gl2}, E_{glo} and η_{glo} are the values of E_1, E_2, η_1, η_2, E_0 and η_0 in the upper left-hand corner of the beam cross-section, respectively. The parameters, μ_i where $i=1,2,...,6$, control the change of E_1, E_2, η_1, η_2, E_0 and η_0, respectively. It should be noted that the exponential laws applied here are commonly used for treating the change of material properties in continuously inhomogeneous (functionally graded) materials.

The SERR, G , for the longitudinal crack (Fig. 2) is determined by analyzing the balance of the energy. In this way, the following expression is derived:

$$G=\frac{1}{h}\left(F\frac{\partial u}{\partial a}-\frac{\partial U}{\partial a}\right), \quad (35)$$

where F is the axial force in the crack arm *1*. The strain energy, U , in the beam is found as

$$U=a\iint_{(A_l)}u_{01}dA+(l-a)\iint_{(A)}u_{02}dA, \quad (36)$$

where A_l and A are the areas of cross-sections of the crack arm *1* and the beam. The strain energy density, u_{01}, in crack arm *1* is determined as

$$u_{01}=\int_0^{\varepsilon}\sigma d\varepsilon . \quad (37)$$

Here, σ is obtained by using (25). The strain energy density, u_{02}, in the beam portion, $a\le x_1\le l$, is derived by replacing of σ with σ_{unc} in (37). The stress, σ_{unc}, in the beam portion, $a\le x_1\le l$, is found by replacing of ε with ε_{unc} in (25). Here, ε_{unc} is the strain in beam portion, $a\le x_1\le l$.

The distributions of ε and ε_{unc} in the cross-sections of the crack arm *1* and the beam portion, $a\le x_1\le l$, are written as

$$\varepsilon=\varepsilon_{C_2}+\kappa_{y_2}y_2+\kappa_{z_2}z_2, \quad (38)$$

$$\varepsilon_{unc}=\varepsilon_{C_3}+\kappa_{y_3}y_3+\kappa_{z_3}z_3, \quad (39)$$

where z_2 and y_2 are the centric axes of crack arm *1*, z_3 and y_3 are the centric axes of the beam portion, κ_{y_2} and κ_{z_2} are the curvatures of the crack arm *1*, κ_{y_3} and κ_{z_3} are the curvatures of the beam portion, ε_{C_2} and ε_{C_3} are the strains in the centers of cross-sections of the crack arm *1* and the beam portion, respectively.

The curvatures and the strains in the centers of the cross-sections are determined from the equations

$$\iint_{(A_l)}\sigma z_2 dA=0, \quad (40)$$

$$\iint_{(A_l)}\sigma y_2 dA=0, \quad (41)$$

$$\iint_{(A)}\sigma_{unc}z_3 dA=0, \quad (42)$$

$$\iint_{(A_l)}\sigma dA=\iint_{(A)}\sigma_{unc}dA, \quad (43)$$

$$\iint_{(A_l)}\sigma\left(y_2-\frac{b_2}{2}\right)dA=\iint_{(A)}\sigma_{unc}y_3 dA, \quad (44)$$

$$u=\varepsilon_{C_2}a+\left[\varepsilon_{C_3}+\kappa_{y_3}\left(-\frac{b_2}{2}\right)\right](l-a). \quad (45)$$

Equations (40), (41) and (42) are obtained by using the fact that the bending moments about the centric axes of the crack arm *1*, and the bending moment about the horizontal centric axis of the intact beam portion are zero. Equation (43) expresses the equilibrium of the axial forces in the crack arm *1* and in the intact beam portion. Equation (44) is obtained by considering the equilibrium of bending moments about the vertical centric axis the intact beam portion. Equation (45) is derived by calculating of the displacement, u, by the integrals of Maxell-Mohr. After substituting of stresses in (40) – (45), equations (40) – (45) are solved with respect to κ_{y_2} , κ_{z_2} , κ_{y_3} , κ_{z_3} , ε_{C_2} and ε_{C_3} .

By combining of (35), (36) and (45), one obtains

$$G=\frac{1}{h}\left[F\left({}_{C_2}-\varepsilon_{C_3}+\kappa_{y_3}\frac{b_2}{2}\right)-\iint_{(A_l)}u_{01}dA+\iint_{(A)}u_{02}dA\right] \quad (46)$$

The integration in (46) is performed by the MatLab.

The solution of the SERR (46) is verified by applying the method of the *J*-integral [18]. The contour, H, is used (Fig. 2). The *J*-integral is

$$J_{av}=\frac{1}{h}\int_{-\frac{h}{2}}^{\frac{h}{2}}\left\{\int_{H_1}\left[u_{01}\cos\alpha-\left(p_x\frac{\partial u}{\partial x}+p_y\frac{\partial v}{\partial x}\right)\right]ds+\int_{H_2}\left[u_{02}\cos\alpha_{H_2}-\left(p_{x_{H_2}}\frac{\partial u}{\partial x_{H_2}}+p_{y_{H_2}}\frac{\partial v}{\partial x_{H_2}}\right)\right]ds_{H_2}\right\}dz_1 . \quad (47)$$

The integrals in (47) are solved by the MatLab. The *J*-integral matches the SERR which is a check-up of the solution.

3. Results

The results presented in this section of the paper are obtained by applying the solution of SERR (47). It is assumed that $b=0.012$ m, $h=0.018$ m, $l=0.300$ m and $\nu_g=0.004\times10^{-8}$ m/sec^2.

Figure 3 shows how the evolution of the dimensionless SERR with dimensionless time is affected by the value of the parameter, μ_1. The following formulae are applied to present the SERR and time in dimensionless form: $G_N=G/(E_{gl1}b)$ and $t_N=tE_{gl1}/\eta_{gl1}$. Examination of Fig. 3 shows a decrease in SERR upon growth of μ_1, which is explained with increase of beam stiffness.

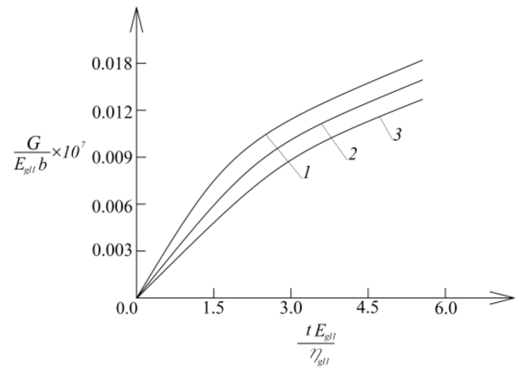

Figure 3. The SERR presented as a function of time (curve 1 – at $\mu_1 = 0.5$, curve 2 – at $\mu_1 = 1.0$ and curve 3 – at $\mu_1 = 2.0$)

The influence of parameter, v_g, on the SERR at three values of the parameter, μ_3, is illustrated in Fig. 4. It is evident from curves in Fig. 4 that when v_g increases, the SERR also increases (this is a result of increase of axial displacement).

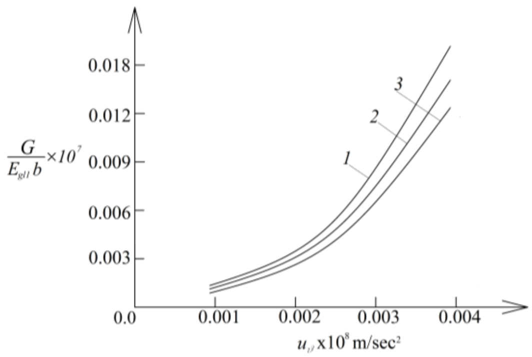

Figure 4. The SERR presented as a function of v_g (curve 1 – at $\mu_3 = 0.5$, curve 2 – at $\mu_3 = 1.0$ and curve 3 – at $\mu_3 = 2.0$)

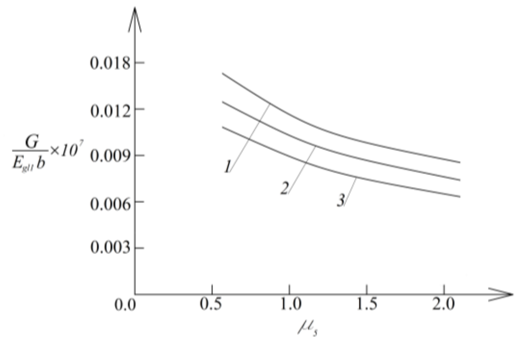

Figure 5. The SERR presented as a function of μ_5 (curve 1 - at $\mu_6 = 0.5$, curve 2 - at $\mu_6 = 1.0$ and curve 3 - at $\mu_6 = 2.0$)

One can observe that increase of the parameter, μ_3, causes reduction of the SERR (Fig. 4).

One can evaluate the effect of the continuous change of E_0 and η_0 from Fig. 5 where the SERR is plotted against μ_5 at three values of μ_6. Figure 5 reveals that the SERR reduces with increasing of the parameters, μ_5 and μ_6 (this is due to increase of the structure rigidity).

4. Conclusion

The SERR for a longitudinal crack in a non-linear viscoelastic beam configuration exhibiting two-directional continuous material inhomogeneity in its cross-section is analyzed. The crack arm *1* is loaded in tension so as the axial displacement increases continuously with time. A non-linear viscoelastic mechanical model having four linear and two non-linear components is used for describing of the time-dependent behavior of the beam structure. The material properties (modules of elasticity and coefficients of viscosity) are distributed continuously along both width and thickness of the beam. The SERR is derived by analyzing the balance of the energy. The method of the *J*-integral is applied to check-up the solution of the SERR. The influence of the two-directional material inhomogeneity on the SERR is assessed by varying the parameters characterizing the change of the material properties in the beam cross-section. It is found that the SERR reduces when the parameters, μ_1, μ_3, μ_5 and μ_6, increase. It is found also that increase of v_g results in growth of SERR. It should be emphasized that the mathematical models in this paper are used mainly to illustrate the way for dealing with longitudinal fracture problem in non-linear viscoelastic beams with two-dimensional material inhomogeneity. For various specific problems that may be encountered in engineering practice, unique models must be developed and applied in the analysis of fracture that reflect the specific distribution of material properties in the structure and the regularities of viscoelastic behavior. The practical application of the research presented in this paper is in fracture mechanics based safety design of structures.

Acknowledgements: The paper is a part of the research done within the project BN-326/25. The author would like to thank the Research and Development Centre (CNIP) for the financial support.

References

1. K. Li, M. Zhang, Z. Zhang, P. Jin, Y. Wang, W. Yan, L. Zhu, D. Zhang, L. Murr, “High performance realization of functionally graded materials based on integrated optimal design and additive manufacturing: A review”, *International Materials Reviews*, vol. 70, no. 6, pp. 497-547, 2025. https://doi.org/10.1177/09506608251354889
2. I.M. El-Galy, B.I. Saleh, M.H. Ahmed, “Functionally graded materials classifications and development

trends from industrial point of view, *SN Appl. Sci.*, vol. 1, pp. 1378, 2019. https://doi.org/10.1007/s42452-019-1413-4

3. Z. Hu, Z. Ma, L. Yu, Y. Liu, "Functionally graded materials with grain-size gradients and heterogeneous microstructures achieved by additive manufacturing", *Scripta Materialia*, vol. 226, 115197, 2023. https://doi.org/10.1016/j.scriptamat.2022.115197
4. Q. Chen, J. Lai, Y. Ye, Y. Tian, S. Guo, J. Zhang, "A simple and effective strategy for WCu functionally graded materials with continuous gradient", *International Journal of Refractory Metals and Hard Materials*, vol. 128, 106974, 2025. https://doi.org/10.1016/j.ijrmhm.2024.106974
5. H.S. Hedia, S.M. Aldousari, A.K. Abdellatif, N.A. Fouda, "New design of cemented stem using functionally graded materials *(FGM)"*, *Biomed. Mater. Eng.*, vol. 24, no. 3, pp. 1575-1588, 2014. https://doi.org/10.3233/BME-140962
6. N. Van Thinh, H. Van Tung, "Free Vibration and Dynamical Analyses of FGM Plates with Porosity and Tangential Edge Constraints", *J. Vib. Eng. Technol.*, vol. 12, pp. 5291–5305, 2024. https://doi.org/10.1007/s42417-023-01205-y
7. Vu Thanh Long, Hoang Van Tung, "Thermo-torsional buckling and postbuckling of thin FGM cylindrical shells with porosities and tangentially restrained edges", *Mechanics Based Design of Structures and Machines*, vol. 51, no. 12, pp. 7056-7075, 2023. https://doi.org/10.1080/15397734.2022.2084752
8. N. Van Thinh, H. Van Tung, "Nonlinear vibration of geometrically imperfect CNT-reinforced composite cylindrical panels exposed to thermal environments with elastically restrained edges", *Acta Mech*, vol. 235, pp. 1147–1164, 2024. https://doi.org/10.1007/s00707-023-03791-0
9. L. Tokova, A. Yasinskyy, C.-C. Ma, "Effect of the layer inhomogeneity on the distribution of stresses and displacements in an elastic multilayer cylinder", *Acta Mechanica*, vol. 228, pp. 2865-2877, 2017. https://doi.org/10.1007/s00707-015-1519-8
10. K. Bousmaha, S. A. Belalia, S. M. Chorfi, A. Tounsi, M. A. Al-Osta, A. E. Alluqmani, "On the dynamic behavior of plates made of porous advanced materials reinforced with carbon nanotubes using a *p*-version of finite element method", *Mechanics Based Design of Structures and Machines*, pp. 1–30, 2025. https://doi.org/10.1080/15397734.2025.2534679
11. A. Tounsi, Z. Belabed, F. Bounouara, M. Balubaid, S.R. Mahmoud, A.A. Bousahla, A. Tounsi, "A finite element approach for forced dynamical responses of porous FG nanocomposite beams resting on viscoelastic foundations", *Int. J. Struct. Stab. Dyn.*, 2650078, 2024. https://doi.org/10.1142/S0219455426500781
12. R. M. Mahamood, E. T. Akinlabi, "Future Research Direction in Functionally Graded Materials and Summary," In: *Functionally Graded Materials. Topics in Mining, Metallurgy and Materials Engineering*, Springer, Cham, 2017. https://doi.org/10.1007/978-3-319-53756-6_6
13. V. Rizov, "Delamination analysis of inhomogeneous viscoelastic beam of rectangular section subjected to torsion", *Coupled Systems Mechanics*, vol. 12, no. 1, pp. 69-81, 2023. https://doi.org/10.12989/csm.2023.12.1.069
14. V. Rizov, "Effects of Periodic Loading on Longitudinal Fracture in Viscoelastic Functionally Graded Beam Structures", *J. Appl. Comput. Mech.*, vol. 8, no. 1, pp. 370–378, 2022. https://doi.org/10.22055/JACM.2021.37953.3141
15. Z.-H. Wang, L. Zhang, L.-C. Guo, "A viscoelastic fracture mechanics model for a functionally graded materials strip with general mechanical properties," *European Journal of Mechanics - A/Solids*, vol. 44, pp. 75-81, 2024. https://doi.org/10.1016/j.euromechsol.2013.10.008
16. M. Ciavarella, A. Papangelo, R. McMeeking, "Transient and steady state viscoelastic crack propagation in a double cantilever beam specimen", *International Journal of Mechanical Sciences*, vol. 229, 107510, 2022. https://doi.org/10.1016/j.ijmecsci.2022.107510
17. F. Pan, W. Li, B. Wang, X. Zhang, "Viscoelastic fracture of multiple cracks in functionally graded materials", *Computer Methods in Applied Mechanics and Engineering*, vol. 198, no. 33-36, pp. 2643-2649, 2009. https://doi.org/10.1016/j.cma.2009.03.005
18. D. Broek, "Elementary engineering fracture mechanics," Springer, 1986.